Zener Polaron Ordering in Half-Doped Manganites

A. Daoud-Aladine,[1] J. Rodríguez-Carvajal,[1,2] L. Pinsard-Gaudart,[1,3] M. T. Fernández-Díaz,[4] and A. Revcolevschi[3]

[1]*Laboratoire Léon Brillouin, CEA-CNRS Saclay, 91191 Gif sur Yvette, France*

[2]*Service de Physique Statistique Magnétisme et Supraconductivite, CEA, 38054 Grenoble, France*

[3]*Laboratoire de Physico-Chimie de l'Etat Solide, Université Paris Sud, Bâtiment 414, 91405 Orsay, France*

[4]*Institut Laue-Langevin, 38042 Grenoble, France*

(Received 20 April 2001; published 13 August 2002; publisher error corrected 3 September 2002)

We have refined the crystal structures of a $Pr_{0.60}Ca_{0.40}MnO_3$ single crystal from neutron diffraction data. The result at low temperature gives a superstructure that cannot be interpreted as Mn^{3+}/Mn^{4+} charge ordering. The pattern of atom displacements suggests the trapping of electrons within pairs of Mn sites, involving both a local double exchange and a polaronic-like distortion. The two mechanisms act together to form vibronic localized electronic states: Zener polarons. We have confirmed this picture by showing how it elucidates the unconventional paramagnetic behavior of half-doped manganites.

DOI: 10.1103/PhysRevLett.89.097205 PACS numbers: 75.30.Vn, 61.12.–q, 71.27.+a, 71.30.+h

Half-doped manganites $R_{1/2}Ca_{1/2}MnO_3$ (R: trivalent ion like Bi, La, Pr, Sm, Y) display a unique magnetic signature. It is an antiferromagnetic (AF) arrangement of ferromagnetic (F) Mn zigzag chains below the Néel temperature T_N, known as the CE-type structure [1]. Goodenough has shown that these AF properties are well understood within the superexchange theory. As half-doped manganites have a mixed valence, the scheme of the orbital ordering (OO) of the Mn^{3+} d_{z^2} orbitals explaining the CE structure is concomitant to a charge order (CO) pattern of Mn^{3+}/Mn^{4+} ions [2]. Let us recall that historically, the Goodenough model (GM) of OO/CO for manganites has contributed to the setting up of the Goodenough-Kanamori-Anderson (GKA) rules for the superexchange interaction. But it is only later that the GKA rules have shown they allow a coherent description of the AF properties of many transition metal insulating compounds [3]. In this sense, the description of the electronic states in half-doped manganites, as ionic Mn^{3+} and Mn^{4+} states, cannot be totally justified just by the fact that their magnetic structure is consistent with the GKA rules applied to a CO/OO model.

However, such CO and OO models have promoted the idea that the structure-transport relationships in doped manganites are strongly influenced by the dynamic fluctuations of the Mn-O bond lengths in the high temperature (HT) semiconducting phase. The dominant electron-phonon coupling mechanisms are believed to be breathing type distortions of the MnO_6 octahedron that stabilize a Mn^{4+} small polaron, or a Jahn-Teller (JT) type distortion around the Mn^{3+} sites. Below a transition temperature, the static ordering these Mn-O bond lengths can accompany the electronic localization. The GM model of CO/OO seems to be justified in the $R_{1/2}Ca_{1/2}MnO_3$ compounds displaying a structural transition at low temperature (LT), below $T_{CO} \geq T_N$. It is evidenced by the onset of the superstructure reflections in the electron, x-ray and neutron diffraction patterns, that are indexed by the $\mathbf{q}_{CO} = (0, \frac{1}{2}, 0)$ propagation vector with respect to the HT cell of $Pbnm$ symmetry [4–7].

It has been further shown that this commensurate modulation does not necessarily require the exact $x = 1/2$ doping level. In the $Pr_{1-x}Ca_xMnO_3$ system it is even stable down to the $x \approx 0.3$ doping level [4,8,9]. Such $1/3 < x < 1/2$ compounds present a variant of the AF-CE spin ordering, called pseudo-CE-type. Within the frame of the GM, they can be considered as having an excess of Mn^{3+} ions, with respect to the ideal $x = 1/2$ doping. These excess electrons are accommodated in the 1:1 Mn^{3+}/Mn^{4+} commensurate ordering of the CE motif, where they are supposed to place randomly on the Mn^{4+} sites [10]. Hence these extra Mn^{3+} ions can be considered as structural defects, and the average charge ordered structure should be fundamentally the same for all $1/3 < x < 1/2$. The change ordered pattern is then supposed to be formed by alternating Mn^{3+} and Mn^{4+} strings along **c** in the (**a**, **b**) plane of the Mn lattice.

The expected distortions of GM model can be experimentally checked by a detailed structure determination of any compound presenting a commensurate $\mathbf{q}_{CO} = (0, \frac{1}{2}, 0)$ structural modulation. Unfortunately, all single crystals manganite samples present a twinned structure making the analysis more difficult. At present, the only available solutions proposed to date for the charge ordered structure was obtained from the refinement of powder diffraction data [8,10–13], following the pioneering work of Radaelli *et al.* [5]. All these studies propose the same monoclinic $P112_1/m$ symmetry, with a doubled cell along **b** in the $Pbnm$ setting, for the LT phase. The single crystal structure determination of a charge ordered phase was recently published, but in a bi-layered manganite $LaSr_2Mn_2O_7$ [14] where the mismatch between the perovskite and NaCl-like (La,Sr)O layers introduce additional distortions. The conclusion of the authors is that despite a very similar Mn-O distances for the two sites, the pattern of distortions is similar to that found by Radaelli *et al.* [5].

It is empirically well established by the Bond valence model (BVM) [15], that a Mn^{3+}/Mn^{4+} CO should result in

the setting up of MnO_6 octahedra with very different average Mn-O distances. Note that in $LaMnO_3$ (Mn^{3+}) and $CaMnO_3$ (Mn^{4+}), these $d_{\text{Mn-O}}$ distances are 2.02 and 1.90 Å, respectively. In the half-doped Mn perovskites, none of the BVM calculations, carried from the cited diffraction studies, is able to confirm this expectation. Hence, these structure refinements can only be, at the best, interpreted as if there was a partial CO of the type $Mn^{+3.5+\delta}/Mns^{+3.5-\delta}$. In this model, the refined structure shows that half of the Mn sites, on which the $P112_1/m$ symmetry already imposes an inversion center, are in elongated oxygen octahedra. These sites are considered as Mn^{+3} ions only because they present a JT-like distortion.

In this Letter, we report a complete structure refinement of a $Pr_{0.60}Ca_{0.40}MnO_3$ single crystal. Two data collections were performed using the 2D detector of the four circle diffractometer D9 at the Institute Laue-Langevin in Grenoble above and below $T_{CO} = 235$ K. The characterization of a crushed piece of the same crystal using synchrotron high resolution powder diffraction (SHRPD at BM16-ESRF, Grenoble) and transmission electron microscopy (TEM, at CRISMAT, Caen) shows that the crystal is greatly homogeneous. TEM lattice images at 92 K shows the structural modulation is perfectly long range order, the system of fringes does not display any kind of visible defects below a scale larger than 1000 Å. This indicates also that the twinning in this $Pr_{0.60}Ca_{0.40}MnO_3$ single crystal is macroscopic. The calcium composition has been determined to be homogeneous by EELS to be within the range $x = 0.39 \pm 0.02$. The technical details of the neutron diffraction data collection and refinements of the twinned crystal data is out of the scope of this Letter, and will be published elsewhere.

At $T = 280$ K the refined structure has an orthorhombic $Pbnm$ symmetry. It is very similar to the already published data [4]. The cell parameters (SHRDP data) are $a = 5.4210(1)$ Å, $b = 5.4460(1)$ Å, and $c = 7.6480(1)$ Å. It has a unique Mn site and displays a pattern made of tilted nearly regular octahedra, whose $d_{\text{Mn-O}}$ is characteristic of an intermediate valence site (see Table I).

Below T_{CO} at $T = 195$ K, group theory gives six possible isotropy subgroups of the HT phase $Pbnm$ symmetry, that have a doubled cell along **b**. Keeping **c** as the unique axis, these are the $P11m$, $P2_1nm$, $P112_1/m$, $P112_1/b$, $P2_1nb$, and $P11b$ space groups. The measured diffraction intensities mix the different domain contribution. Using a twin law and a common structural model for the six domains of the twinned crystal we performed a full refinement of the collected data, refining all of the possible structural positional parameters in each isotropy subgroups symmetry. The best results are obtained using the $P2_1nm$ and $P11m$ space groups. Both of them describe structures with almost the same atomic positions, indicating a strong orthorhombic $P2_1nm$ pseudosymmetry, since $P11m$ is a subgroup of $P2_1nm$. The previously proposed $P112_1/m$ symmetry [5] fails to take into account all the 722 measured intensities of the superstructure lines of our crystal (see Fig. 1). We conclude that LT phase has $P11m$ symmetry because SHRPD data shows a monoclinic cell. But the refined structural parameters are more conveniently described by the $P2_1nm$ pseudosymmetry. They are displayed in Table II. A schematic pattern of the atomic displacements in this LT phase is depicted in Fig. 2(a).

The refined structure presents two Mn sites but the geometrical characteristics discussed below are inconsistent with Mn^{3+}/Mn^{4+} CO. Even if they would have carried different charges, the way these sites alternate along the **b** direction would give a different Mn^{3+}/Mn^{4+} charge ordered pattern than the GM model. The intermediate valence state for the Mn atoms in this structure is anyway confirmed by the very similar $d_{\text{Mn-O}}$ of the two Mn sites (see Table I). This agrees with the suggestion of an intermediate valence state for Mn at all temperatures in the half-doped charge ordered manganites, coming from the study of the XANES at the Mn K-edge of $La_{1/2}Ca_{1/2}MnO_3$ [17]. The structure is not incompatible with the onset of

TABLE I. Octahedral distortions in $Pr_{0.60}Ca_{0.40}MnO_3$. $\Delta = \frac{1}{6}\sum_{i=1}^{6} \left|\frac{d_{\text{MnO}_i} - \langle d_{\text{MnO}}\rangle}{\langle d_{\text{MnO}}\rangle}\right|^2$ measure the octahedral distortion. The bond valence sums (BVS), uses the Mn^{3+} d_0 parameter for all sites (see Ref. [16] for definitions).

$T = 280$ K	$T = 195$ K	
Mn site	Mn_1 site	Mn_2 site
Mn-O_{ap} : 1.953(1)(×2)	Mn_1-O'_1 : 1.951(3)	Mn_2-O'_3 : 1.957(3)
Mn-O_{eq} : 1.967(2)(×2)	Mn_1-O'_2 : 1.942(3)	Mn_2-O'_4 : 1.940(3)
Mn-O_{eq} : 1.953(1)(×2)	Mn_1-O_1 : 1.879(2)	Mn_2-O_4 : 1.899(2)
	Mn_1-O_1 : 2.053(2)	Mn_2-O_4 : 2.028(2)
	Mn_1-O_3 : 1.980(2)	Mn_2-O_3 : 2.011(2)
	Mn_1-O_2	Mn_2-O_2 : 1.899(2)
$d_{\text{Mn-O}} = 1.957(1)$ Å	$d_{\text{Mn-O}} = 1.960(1)$ Å	$d_{\text{Mn-O}} = 1.955(1)$ Å
BVS = 3.52	BVS = 3.53(1)	BVS = 3.50(1)
$\Delta(\times 10^{-4}) = 0.12$	$\Delta(\times 10^{-4}) = 6.99$	$\Delta(\times 10^{-4}) = 6.506$

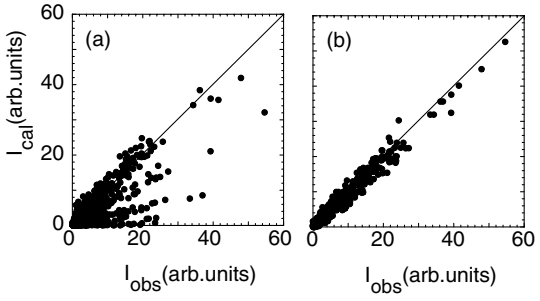

FIG. 1. Observed vs calculated intensity of superstructure lines indexed as $(h, k + 1/2, l)$ in the HT cell setting, in $Pr_{0.60}Ca_{0.40}MnO_3$ with $P112_1/m$ (a) and $P2_1nm$ symmetry (b) structural models. Reliability factors of the refinements are as follows: for $P112_1/m$ symmetry, $R^f_{F^2} = 4.21\%$ for the 827 measured fundamental lines, and $R^{ss}_{F^2} = 39.3\%$ for 722 superstructure lines; using the $P2_1nm$ symmetry $R^f_{F^2} = 2.62\%$ and $R^{ss}_{F^2} = 10.8\%$.

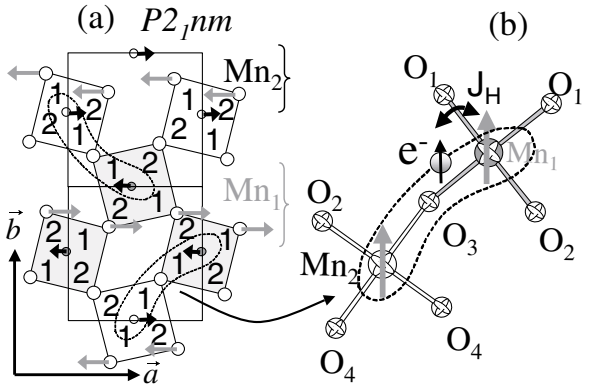

FIG. 2. MnO_2 (a),(b) planes of the structure: (a) schematic representation of the displacements of the atoms with respect to their average $Pbnm$ positions, that are exaggerated for clarity, in the $P2_1nm$ symmetry. Labels "1" and "2" stand for long (≈ 2 Å) and short (≈ 1.9 Å) Mn-O distances. (b) the Zener polaron: arrows are $S = 3/2$ localized magnetic moments coupled by the DE of one electron.

"forbidden" reflections in resonant x-ray scattering (RXS) at the Mn K-edge experiments. Previous studies have, however, often taken them as a proof of Mn^{3+}/Mn^{4+} charge ordering [18]. This confirms that the correct interpretation of of RXS data must consider other mechanisms than uniquely the splitting of Mn 3d electronic states by a charge gap [19]. It has also been shown that some specific octaedral distortions can explain the observed polarization dependence of the forbidden resonant reflections intensity, without necessarily invoking that they arise from different charge densities around the Mn atoms [20].

If Mn keeps an intermediate valence state, it should be asked what is the driving mechanism for the electron localization. To get the answer let us describe first some features of the refined structure that suggest a Mn_1-Mn_2 pairing [see Fig. 2(a)]. The most obvious distortion of this LT structure is that Mn_1O_6 and Mn_2O_6 form pairs of octahedra that are elongated in the same direction. This common elongation direction and the off-centering of Mn_1 and Mn_2 strongly suggest a Mn_1-Mn_2 dimerization phenomenon. This occurs together with the opening of the Mn_1-O_3-Mn_2 angle, which becomes the widest angle in the LT structure (159°). The octahedral distortion with respect to the HT phase evidence an anisotropic charge redistribution. The extra electron per pair of core Mn^{4+} is likely to be easily delocalized on the pair by the opening of the Mn_1-O_3-Mn_2 angle. Such a fast electron transfer, leading to the formation of Mn-Mn dimers, has already been proposed by Zhou and Goodenough, to the explain the specific transport properties of the different F phases of a $La_{1-x}Sr_xMnO_3$ $x = 0.14$

TABLE II. Refinement of structural parameters of $Pr_{0.60}Ca_{0.40}MnO_3$ at $T = 195$ K in the orthorhombic $P2_1nm$ pseudosymmetry, the real structure is moniclinic $P11m$, with cell parameters $a = 5.4315(1)$ Å, $b = 10.8970(2)$ Å, $c = 7.6370(1)$ Å, $\gamma = 90.076(2)°$. The doubled cell origin is shifted by a (0 3/4 1/4) translation with respect to the high temperature orthorhombic $Pbnm$ phase.

Atom	Wyck. Pos.	x	y	z	B_{iso} (Å^2)
Pr/Ca_1	2a	0.5121(4)	0.8936(2)	0	0.53(3)
Pr/Ca_2	2a	0.4784(4)	0.3614(2)	1/2	0.77(3)
Pr/Ca_3	2a	−0.0023(4)	0.1426(2)	0	0.56(3)
Pr/Ca_4	2a	0.9905(4)	0.6088(2)	1/2	0.25(2)
Mn_1	4b	0	0.8756(2)	0.2489(3)	0.31(2)
Mn_2	4b	0.9795(2)	0.3746(1)	0.7492(4)	0.13(2)
O_1	4b	0.3044(4)	0.9845(1)	0.2861(2)	0.26(2)
O_2	4b	0.7090(4)	0.2676(1)	0.7891(2)	0.48(1)
O_3	4b	0.2112(4)	0.2328(1)	0.7148(2)	0.96(2)
O_4	4b	0.7515(4)	0.5191(1)	0.2110(2)	0.41(2)
O'_1	2a	0.4353(4)	0.1125(2)	0	0.41(2)
O'_2	2a	0.5743(4)	0.1321(2)	1/2	0.68(3)
O'_3	2a	0.0562(4)	0.3758(1)	0	0.33(2)
O'_4	2a	0.9104(4)	0.3846(2)	1/2	0.69(2)

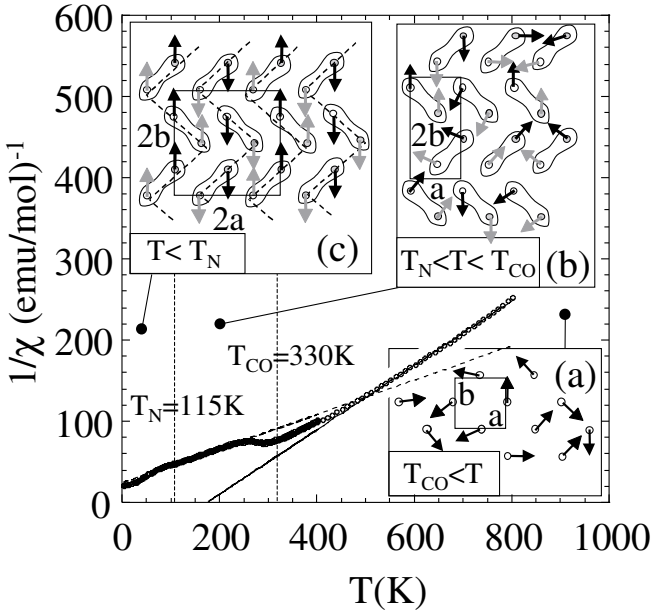

FIG. 3. χ^{-1} vs T of the magnetic susceptibility of $Y_{1/2}Ca_{1/2}MnO_3$. A schematic picture of the magnetic state of the compound is shown in the inset: (a) PM above T_{CO}; (b) PM Zener polaron order between T_{CO} end T_N; (c) AF-CE structure below T_N.

crystal under pressure [21]. They called this dimer a ''Zener polaron'' (ZP) because the easy delocalization should be associated to the double exchange (DE) Zener mechanism that couples ferromagnetically both Mn ions in the pair [see Fig. 2(b)]. The LT refined structure, which is an average description of the $Pr_{0.60}Ca_{0.40}MnO_3$ studied crystal, may be viewed as a commensurate Zener polarons ordering (ZPO) in the (**a**, **b**) plane [see Fig. 3(b)] inviting us to consider that it is in fact the ideal ZPO of the parent $Pr_{1/2}Ca_{1/2}MnO_3$ compound. The stability of the ZPO structure is assured by the structural distortion favoring a local/confined DE process.

The ZPO gives also a clue to interpret the anomaly in the magnetic susceptibility that is observed at T_{CO}, while samples are remaining in a paramagnetic (PM) state. The change in the magnetic correlations that vary from F to AF on lowering the temperature below T_{CO} [22], fits very well within the proposed ZPO model. The F correlations at HT is a consequence of disordered and dynamic DE. Their disappearance is not due to the ''switch off'' of DE, as it is commonly accepted in the atomic CO/OO picture, but to the ''switch on'' of AF correlations because the ZPO changes the nature of the paramagnetic units: below T_{CO} the new units are ferromagnetic pairs, so that the effective moment should also be modified.

Above T_{CO}, there are N sites of paramamagnetic ions of effective moment $\bar{\mu}_{\text{eff}} = (1/2\mu^2_{Mn^{3+}} + 1/2\mu^2_{Mn^{4+}})^{1/2} = 4.41\mu_b$. ZP formation should lead to $N/2$ new elemental paramagnetic units of effective moment $\mu_p = 2[S(S+1)]^{1/2} = 7.94\mu_b$ ($S = 7/2$). Hence it is predicted that the Curie constant $C = N\mu^2_{\text{eff}}/k_B$, increases by a factor given by $C_{LT}/C_{HT} = 1.62$, where C_{HT} and C_{LT} are the Curie constant above T_{CO} and between T_{CO} and T_N. We have measured the magnetic susceptibility of the half-doped CO $Y_{1/2}Ca_{1/2}MnO_3$ compound with a SQUID device up to $T = 400$ K and in the range $T = 300$ K to $T = 800$ K with a Faraday balance. The data, and the refinement of the asymptotic Curie-Weiss behavior in the two PM regions, is displayed in Fig. 3 where we have included an artist's scheme of the magnetic moment arrangement in the three relevant temperature regions. We find experimentally on this $Y_{1/2}Ca_{1/2}MnO_3$ compound $C_{LT}/C_{HT} = 1.51$, value that is very close to our prediction. The detailed discussion about the magnetic ordering of the ZP will be published elsewhere.

In conclusion, the present study has allowed us to obtain precise octahedral distortions that are different from those expected for the CO/OO model proposed early by Goodenough. The interpretation of the structure leads to the main point of this work: the formation and ordering of ZP may be an important clue to understanding the electronic localization in half-doped manganites. The extension of this picture to other dopings is appealing. The clearest example is the compound $La_{1/3}Ca_{2/3}MnO_3$ in which the magnetic structure can be described by the AF arrangement of ferromagnetic trimers [23].

[1] E. O. Wollan *et al.*, Phys. Rev. **100**, 545 (1955).
[2] J. B. Goodenough, Phys. Rev. **100**, 564 (1955).
[3] J. Kanamori, J. Chem. Phys. Solids **10**, 87 (1959).
[4] Z. Jirak *et al.*, J. Magn. Magn. Mater. **53**, 153 (1985).
[5] P. Radaelli *et al.*, Phys. Rev. B **55**, 3015 (1997).
[6] S. Mori *et al.*, Nature (London) **392**, 473 (1998).
[7] C. Chen *et al.*, Phys. Rev. Lett. **83**, 4792 (1999).
[8] Z. Jirak *et al.*, Phys. Rev. B **61**, 1181 (2000).
[9] Y. Tokura *et al.*, J. Magn. Magn. Mater. **200**, 1 (1999).
[10] D. Cox *et al.*, Phys. Rev. B **57**, 3305 (1998).
[11] J. Blasco *et al.*, J. Phys. Condens. Matter **9**, 10 321 (1997).
[12] P. M. Woodward *et al.*, Chem. Mater. **11**, 3528 (1999).
[13] O. Richard *et al.*, Acta Crystallogr. Sect. A **55**, 704 (1999).
[14] D. Argyriou *et al.*, Phys. Rev. B **61**, 15 269 (2000).
[15] I. Brown, Acta Crystallogr. Sect. B **48**, 553 (1992).
[16] J. Rodriguez-Carvajal *et al.*, Phys. Rev. Lett. **81**, 4660 (1998).
[17] J. Garcia *et al.*, J. Phys. Condens. Matter **13**, 3229 (2001).
[18] M. Von-Zimmermann *et al.*, Phys. Rev. Lett. **83**, 4872 (1999).
[19] M. Benfatto, Y. Joly, and C. R. Natoli, Phys. Rev. Lett. **83** 636 (1999)
[20] J. Garcia *et al.*, J. Phys. Condens. Matter **13**, 3243 (2001).
[21] S. Zhou-J and J. Goodenough, Phys. Rev. B **62**, 3834 (2000).
[22] F. Millange *et al.*, Phys. Rev. B **62**, 5619 (2000).
[23] M. T. Fernández-Díaz *et al.*, Phys. Rev. B **59**, 1277 (1999).